JOURNAL OF CATALYSIS 19, 127–140 (1970)

Photoelectric Determination of the Work Function of Gold–Platinum Alloys

R. BOUWMAN AND W. M. H. SACHTLER

Afdeling Heterogene Katalyse, Chemische Laboratoria, Rijksuniversiteit, Leyden, The Netherlands

Received December 29, 1969

Films of platinum, gold, and their alloys were prepared by vapor deposition of the metals—either simultaneously or successively—and subsequent sintering under ultrahigh vacuum. The photoelectric emission of these films was investigated and it was found that equilibrated alloys of compositions within the miscibility gap of the Pt–Au phase diagram possessed identical work functions. This agrees with the expectation, based on thermodynamic and diffusion data, that the gold-rich alloy should envelop crystallites of the coexisting Pt-rich alloy. The work function of the gold-rich alloy is lower than that of gold or that of platinum.

These results are completely analogous to those found previously for the Cu–Ni system. The previously predicted dependence of surface composition on the surrounding gas atmosphere has been experimentally verified.

Carbon monoxide causes an enrichment of the platinum in the surface. This process takes several days at room temperature and may be reversed by pumping off the carbon monoxide at elevated temperature.

INTRODUCTION

In previous work (*1–5*) it was shown that the surface composition of clean copper–nickel alloy films, prepared by evaporation of the metals under ultrahigh vacuum followed by sintering at 200°C, is constant and independent of the bulk composition within the limits of the miscibility gap of this system. For these films the photoelectric work function (*1*), the catalytic activity for certain test reactions (*4, 5*) and the chemisorption of hydrogen per unit of surface area (*4*) were found to be constant. These results were interpreted in terms of a model based on thermodynamic (*6, 7*) and diffusion data (*8, 9*). The model assumes that after sintering the films are built up of crystallites, each of which consists of a kernel of a nickel-rich alloy enveloped by a mantle of a copper-rich alloy. The formation of this peculiar arrangement is a consequence of two essential properties of the copper–nickel system:

1. It possesses a miscibility gap.

2. The diffusion rate of one metal (i.e., copper) is significantly greater than that of the other.

The predictions of this model were recently confirmed for granular copper–nickel alloys by Cadenhead and Wagner (*10*). As the model makes use of simple physical laws, one should also be able to predict the surface composition and hence also the chemisorption behavior of related alloy systems. In this respect the platinum–gold system appears almost ideal for checking the basic principles used. The platinum–gold system is known to possess a wide miscibility gap (*11, 12*) for temperatures below 1258°C as follows from the phase diagram shown in Fig. 1. The system also satisfies the second condition, the diffusion of gold being considerably faster than that of platinum. The Kirkendall effect in Au-Pt alloys was proved and studied by Bolk (*13, 14*).

Although equilibration might be extremely slow for bulk alloys, the results ob-

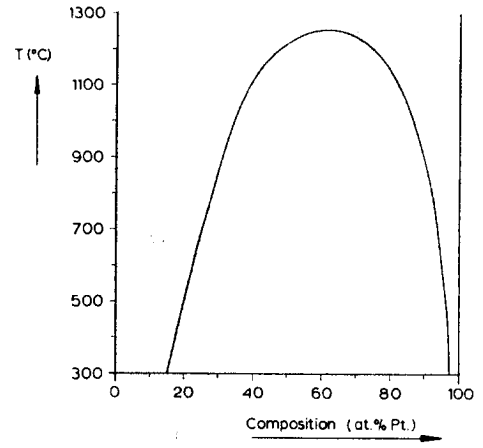

FIG. 1. The phase diagram for gold–platinum alloys.

tained with the copper–nickel system showed that for thin films, prepared under ultrahigh vacuum, equilibration is possible at moderate temperatures. It may, therefore, be expected that for platinum–gold films a surface of constant Pt/Au ratio in the film will be obtained for all alloys with compositions within the miscibility gap. Moreover, we expect that the Pt/Au ratio in the surface should be that of the stable gold-rich alloy at the left-hand edges of the miscibility gap.

In the present article work is described to check these principles. For this purpose platinum–gold alloy films were prepared under ultrahigh vacuum by various techniques including successive and simultaneous vacuum deposition of the two metals followed by sintering. The films obtained were then studied by using them as cathodes in photoelectron emission. In this way each alloy was characterized by its work function ϕ. A second parameter derived from the same measurements is the emission constant M.

Besides the main purpose of checking the two-phase model, for equilibrated films, three additional phenomena are of interest in the present work:

a. For the Cu–Ni system it has been found that the work function is lower for the alloys than both for copper and for nickel. As the present theory of the metallic state does not permit any prediction for the work function of alloys, it appears of interest to explore by experiment whether the work functions of the equilibrated platinum–gold films exhibit a similar minimum.

b. In the Cu–Ni work it appeared possible to "titrate" the surface composition by chemisorption of a gas which is selective for nickel. We thought it worthwhile, therefore, to study the change in work function of platinum–gold films caused by chemisorption of carbon monoxide. This gas is known to be chemisorbed rather strongly by platinum, its heat of adsorption being at least 30 kcal/mole (*15*, *16*), but not by gold, at room temperature.

c. The composition of any alloy surface in thermodynamic equilibrium should, in principle, be dependent upon the surrounding atmosphere. The energy of a Pt/Au–CO system would be lowered by enriching the surface with Pt-atoms which can form strong chemisorption bonds with CO molecules. A dependence of the surface composition on the contacting atmosphere has repeatedly been postulated for alloys (*2*, *17*), but has never been confirmed experimentally. The Cu/Ni–CO system proved to be unsuitable for this purpose because of the formation of gaseous nickel tetracarbonyl on the nickel parts of the cell and the decomposition of this compound on the alloy surfaces causes such a drastic change in the surface composition that a possible simultaneous slow diffusion of metal atoms to the surface cannot be observed. In this respect the Pt/Au–CO system provides much better prospects.

2. Experimental Methods

a. The phototubes

Two types of phototubes have been used. The first one, based on the principle of the phototube used for the copper–nickel system (*1*) is shown in Fig. 2. In this tube (I), successive evaporation of the metals is carried out; whereas in the other phototube (II) (shown in Fig. 4) simultaneous evaporation of both metals is also possible. The first phototube consists of a Pyrex housing (1) having a diameter of 50 mm. Through one end, two elongated parallel

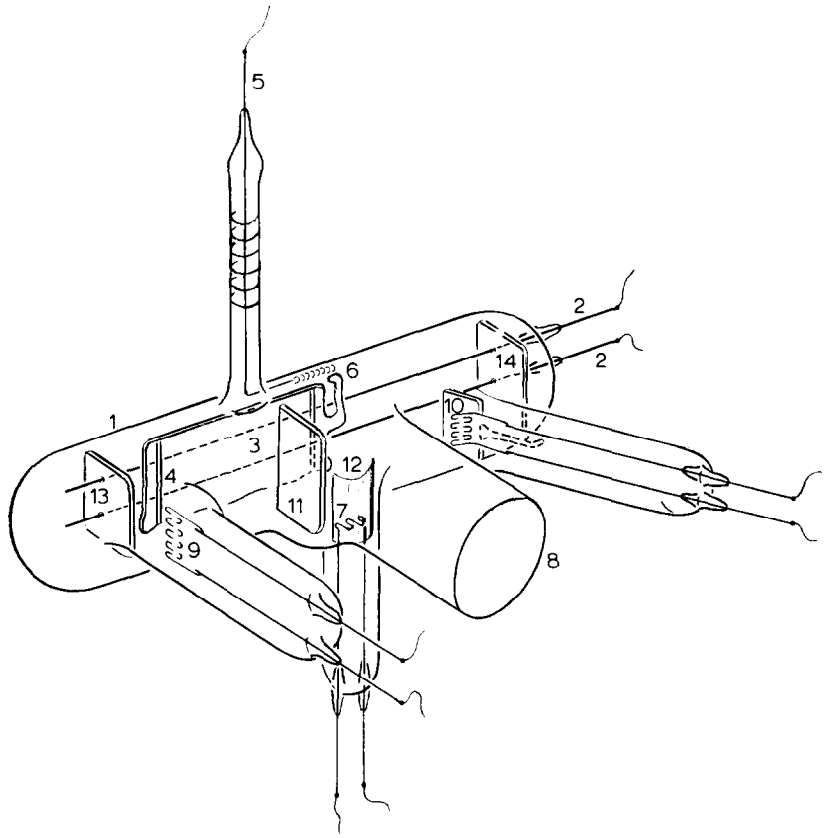

FIG. 2. Phototube, type I.

tungsten rods (2) are fused. A polished Pyrex photocathode (3) sliding over these rods on four small tubes is provided with a glass-clad iron bar in order to make magnetic operation possible from the exterior. The surface of the cathode, to be coated with the alloy films, is in electrical contact with the tungsten rods through fused platinum rods and spirally wound polished platinum wire embedded in the inner surface of the slide tubes. The cathode surface is provided with two slots (4) having a width of 1 mm and a depth of 1–2 mm, in order to separate film segments from each other (see Fig. 3). These slots prevent lateral diffusion of metal atoms across metal or alloy surfaces between film segments. The anode of the phototube consists of a tungsten rod (5) carrying a small platinum wire (6) embedded at a suitable position in the interior of the phototube. The tungsten rod is surrounded by a double quartz-to-Pyrex transition in order to ensure the extreme insulation required for reliable measurements of photocurrents in the range of 10^{-13}–10^{-15} A. Gold evaporated from the source (7) forms the anode screen in contact with the platinum wire (6) in the upper section of the phototube. A

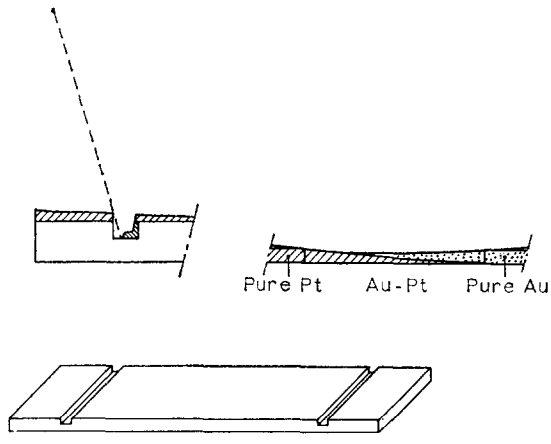

FIG. 3. Details of the photocathode of tube I.

plane parallel quartz window (8) is arranged parallel to the photocathode. The two metal sources (9, 10) are situated on either side of the quartz window with a glass screen (11) to shield part of the cathode during evaporation of one metal. In this way the pure metals are obtained on the terminal zones and a concentration gradient is obtained in the alloys in intermediate positions. A screen (12) protects the quartz window from evaporated gold from source (7). Two screens (13, 14) are placed at the terminals of the tungsten rods (2). Screen (13) serves as a support for the rods, while screen (14) protects the anode and cathode outputs from internal shorting due to the presence of a condensed metal film.

Phototube (II), shown in Fig. 4, used for simultaneous evaporation, consists of a Dewar type tube (1) terminating in a polished cathode (2) provided with similar current-transporting platinum rods (3) fused within the glass and connected to a cathode lead (4). Magnetically movable shutters (5, 6) protect the terminal zones of the cathode which are reserved for the deposition of the pure metals. The anode (7) resembles that of tube (I). The anode metal film in contact with the embedded platinum wire (7) is formed during evaporation of the two metals to be studied. In tube (II) the sequence: gold–alloys–platinum was formed as follows:

1. A small proportion, roughly 10%, of the first metal, [e.g., (8)] is evaporated with shutter (6) in the open position and shutter (5) closed, i.e., pressed flatly onto the cathode.

2. Subsequently, a similar proportion of the other metal (9) is evaporated with the shutter (5) in the open position and shutter (6) closed.

3. Finally, both shutters are closed and the remainder of both metals is evaporated simultaneously. Unfortunately, no slots could be incorporated because of the danger of implosions. (The slot then acts as a notch for rupturing of the cathode, when the tube is evacuated.) Therefore, the whole evaporation process is carried out while cooling the cathode with liquid nitrogen in order

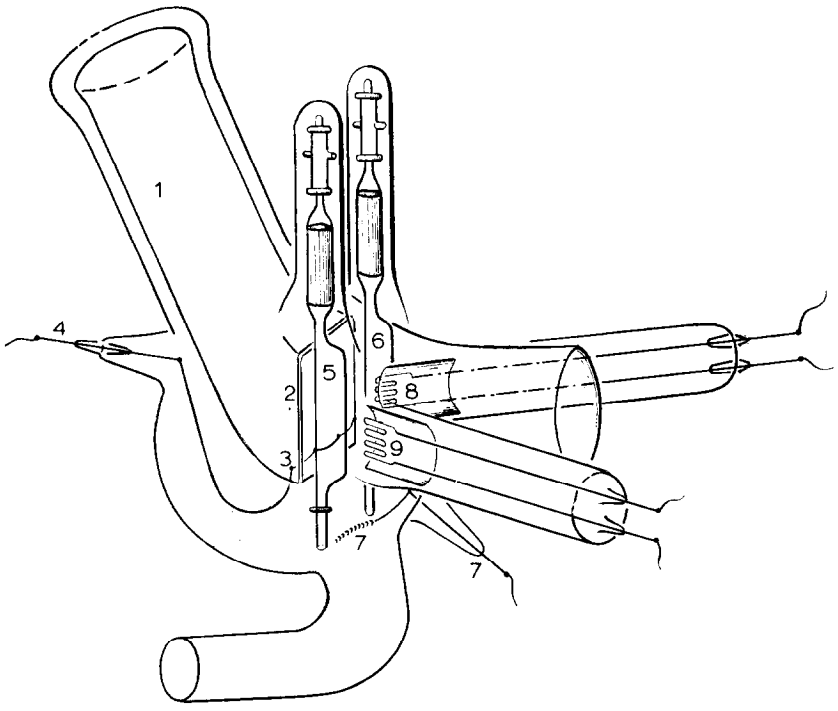

FIG. 4. Phototube, type II.

to prevent the pure metals to become contaminated by premature lateral diffusion. The films in the phototube could be sintered by heating only the cathode by means of a small furnace (not shown) which was pressed against the rear side of the cathode, so that only that part of the phototube was heated during sintering.

b. Metal Deposition

The phototube is connected to an ultrahigh vacuum system evacuated by Edwards rotary and oil diffusion pumps and a Varian Vac-Ion pump. Ultrahigh vacuum is attained by several bakeouts each lasting about 15 hours, at a temperature between 400° and 450°C. Metals are evaporated only when the residual gas pressure is below 3.10^{-10} Torr. Before depositing a film on the photocathode a small proportion of each metal is evaporated while the cathode is shielded completely behind screen (11) (Fig. 1). By means of this preevaporation, volatile impurities are removed so that during subsequent evaporation the pressure will remain below 5.10^{-10} Torr. With gold, it proved difficult to maintain a pressure in the range of 10^{-10} Torr, during evaporation. This metal was therefore pretreated before bakeout by heating it above its melting point in hydrogen at a pressure of 5–10 Torr. This treatment greatly improved the vacuum during the subsequent deposition of gold.

Both metals were evaporated from specially shaped tungsten filaments, spot-welded to tungsten rods. Due to the shape of the filaments, resembling a recurring hairpin, relatively large amounts of platinum could be evaporated without blowing of the filament. Moreover, this special shape had the advantage that very uniform evaporation was achieved in a predictable way. The filaments were always reduced in a hydrogen atmosphere. After the first bakeout-run, the supporting tungsten rods of the filaments were degassed by a high-frequency induction heating until a steady-state pressure below 10^{-8} Torr was recorded. In phototube (I) the cathode was not cooled during film deposition. Due to the heat of radiation from the evaporation sources the local cathode temperature varied between 100 and 200°C depending on the place and the temperature of the source.

In phototube (II) the cathode was always cooled with liquid nitrogen during condensation of the bimetal films.

c. Analysis of the Bulk Composition

The composition pattern on the photocathode was determined by two independent methods:

1. By weighing the filaments before and after evaporation and calculating the distribution of platinum and gold over the cathode from the geometry of the system.

2. By neutron activation analysis. For this purpose, the alloy film strips of interest were dissolved in a small amount of aqua regia prepared from p.a. acids. The solutions were absorbed in ultraclean filtration paper obtained by elution with 0.1 *N* HCl during 20 hr, followed by elution with conductowater during 40 hr, and drying. The analyses were carried out at the Reactor Institute of the Technical University of Delft*. The results of both analytical methods agreed within 5% and were averaged. The removal of the strips of the film from the Pyrex substrate gave rise to the largest errors. We estimated the accuracy of the reported bulk values at about ±3 at. %.

The bulk alloy composition of the cathode was also investigated by X-ray diffraction** in reflection.

d. Determination of the Work Function and the Emission Constant

Light from an air-cooled, high-pressure mercury lamp passing through a Bausch & Lomb grating monochromator was focused via a mirror system onto either the desired location on the photocathode or on a calibrated tantalum reference tube. The photo-

* The authors are indebted to Professor P. J. Houtman and his co-workers for the analysis of the photocathode.

** The authors are very grateful to the contribution of Dr. G. C. Verschoor with regard to these measurements.

current obtained, was amplified by an E.I.L. vibrating reed electrometer, type 51A. The phototubes were coated with a grounded "Aquadag" layer to protect them against external electromagnetic stray fields. Residual fields penetrating to the cathode limited the lower value of reliable measurements of photocurrents to 10^{-14} A. According to the theory of Fowler, the photoelectric yield I in electrons emitted per photon is related to the frequency ν of the light by

$$I = MT^2\left\{\frac{\pi^2}{6} + \frac{x^2}{2} - \left(e^{-x} - \frac{e^{-2x}}{2^2} + \frac{e^{-3x}}{3^2} - \cdots\right)\right\}, \quad (1)$$

where M is the emission constant expressed in electrons photon^{-1} degree^{-2}, T is the absolute temperature and $x = \frac{h\nu - h\nu_0}{kT} = \frac{E - \phi}{kT}$, where ϕ is the work function and $E = h\nu$, the energy per photon, both expressed in electron volts. For $x \gg 1$ or $\nu \gg \nu_0$, (1) becomes to a good approximation:

$$I = \frac{M(E - \phi)^2}{2k^2}. \quad (2)$$

By plotting $I^{1/2}$ against the energy E of the light one obtains ϕ from the intercept on the abscissa and $(M/2k^2)^{1/2}$ as the slope of the straight line. In most instances, the work functions could be evaluated with an accuracy within ± 0.005 eV and the emission constants could be determined with an accuracy of about 1.10^{-12} electrons photon^{-1} deg^{-2}.

The photoelectric yield I is obtained from the recordings of the photocurrents at each frequency by the equation.

$$I = \frac{i_x}{i_{\mathrm{Ta}}} \cdot I_{\mathrm{Ta}}, \quad (3)$$

where i_x is the photocurrent of the unknown metal or alloy, i_{Ta} is the photocurrent of the calibrated tantalum reference tube and I_{Ta} is the photoelectric yield of this reference tube in electrons per photon. Our tantalum tube had been calibrated in the Institut für Physikalische Chemie of the Technische Hochschule, Hannover (W.-Germany) against the standard cells used by Professor Suhrmann, Professor Wedler and their collaborators, to whom we are indebted for providing this opportunity of creating a common standard reference.

3. Results

The results are described in terms of four typical experiments, viz:

I. gold on top of platinum;
II. platinum on top of gold;
III. films prepared by simultaneous deposition of both metals; and

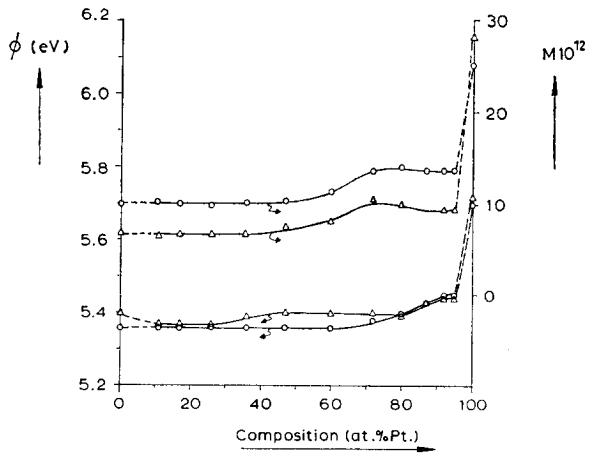

FIG. 5. The work functions (lower curves), and emission constants (upper curves) of a film prepared by evaporating gold on top of platinum (Expt. I): ○, fresh films; △, film sintered at 200°C.

IV. chemisorption of carbon monoxide on alloy films.

Expt. I. Gold on top of platinum. The freshly deposited bimetal films were investigated immediately after evaporation and again after sintering at 200°C during 16 hr. The results are summarized in Table 1 and plotted in Fig. 5. For the fresh films,

TABLE 1
EXPT. I. GOLD ON TOP OF PLATINUM

Pt (at. %)	ϕ_{fresh} (eV)	$M_{fresh} \times 10^{12}$ (electrons/photon × deg²)	$\phi_{sintered}$	$M_{sintered}$
0	5.36	10.1	5.40	6.8
11	5.36	10.3	5.37	6.5
17	5.36	10.1	5.37	6.7
26	5.36	9.9	5.37	6.7
36	5.36	10.2	5.39	6.7
47	5.36	10.4	5.40	7.5
60	5.36	11.4	5.40	8.1
72	5.38	13.7	5.40	10.6
80	5.40	14.0	5.39	10.0
87	5.43	13.7	5.43	8.7
92	5.45	13.7	5.44	9.5
95	5.45	13.7	5.44	9.5
100	5.70	25.1	5.72	28.2

prior to sintering, a gold-like character is detected throughout almost the entire range of alloy compositions. The work function deviates from the gold value only in the region very rich in platinum. After sintering at 200°C, the work function of gold has increased to 5.40 eV while most of the other values have increased slightly. It may be significant that the work functions of some intermediate compositions is now below those of the pure sintered metals. The increase in work function due to sintering of the pure metals is a common phenomenon for most metals, usually explained by assuming that unstable crystal planes and lattice faults disappear from the surface. The increase in work function of some platinum–gold segments can be explained by the same phenomenon of crystallographic ordering and/or to some degree by diffusion of platinum atoms from deeper layers to the surface of the film. Although it is very difficult to derive reliable and easily understandable information from emission constants, which depend on many factors (penetration depths of the photons, escape depth of the electrons, absorption and reflection coefficients, surface area of the film, number and character of dislocation, etc.), the conclusion may be drawn that incomplete equilibration of the film has occurred.

In order to study the effects of lateral diffusion, the work function of Pt was measured in the immediate vicinity of the slot both before and after sintering. While the value, before sintering, was the same on both edges, that of the film in contiguous contact with the composite film showed a lower value after sintering. This is a fair indication for lateral diffusion of gold across the platinum surface. This phenomenon was not detected at the pure gold edge of the cathode. These data suggest that gold diffuses rather easily across the platinum surface, whereas platinum diffusion is not detected. This difference in surface diffusion rates is not surprising; data reported by Bolk (*13*, *14*) also show enhanced diffusion rates for gold in the bulk.

Expt. II. Platinum on top of gold. The results of this experiment are compiled in Table 2 and plotted in Fig. 6. Again a

TABLE 2
EXPT. II. PLATINUM ON TOP OF GOLD

Pt (at. %)	ϕ_{fresh} (eV)	$M_{fresh} \times 10^{12}$ (electrons/photon × deg²)	$\phi_{sintered}$	$M_{sintered}$
0	5.38	6.7	5.38	6.5
12	5.36	14.0	5.34	15.0
19	5.39	14.2	—	—
28	5.42	14.4	5.38	12.5
39	5.41	12.1	5.38	11.7
52	5.40	12.0	5.38	11.7
65	5.42	13.3	5.40	14.4
74	5.49	18.1	5.45	18.8
84	5.60	23.8	5.53	24.6
90	5.70	28.7	5.58	27.1
93	5.75	29.2	5.64	30.0
100	5.70	27.4	5.73	23.6

rather gold-like character is detected at the gold-rich side of the alloy system, but the work function rises sharply from about 60

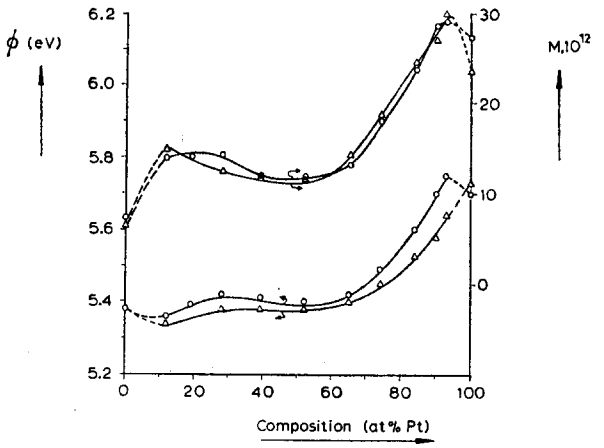

FIG. 6. The work functions (lower curves), and emission constants (upper curves) of a film prepared by evaporating platinum on top of gold (Expt. II): ○, fresh films; △, film sintered at 200°C.

at. % of platinum to pure platinum, with an intermediate maximum at about 95 at. % of platinum. A shallow minimum at about 12 at. % Pt appears prior to sintering. Sintering at 200°C causes effects markedly different from those observed in Expt. I. The work functions of all alloy compositions now *decrease*. The work function of gold remains unchanged and that of platinum increases.

The constancy of the work function of gold upon sintering in Expt. II can be understood as in this case the gold film was exposed to the high heat of radiation during the subsequent deposition of the platinum film. Therefore, the gold film in the "fresh" state is in fact already presintered. Also the fact that the measured value of the nonsintered film at 12 at. % lies below those of pure gold and platinum suggests that some equilibration of the film has been effected, most probably due to the higher heat of radiation during deposition of the second metal, as compared with Expt. I. The observed decrease in work function of the alloys upon sintering in Expt. II is in agreement with our expectation. From the different rates of diffusion it is clear that diffusion from deeper layers of gold (Expt. II) should be faster than that of platinum (Expt. I). The emission constant shows hardly any dependence upon the alloy composition. Sintering at 200°C did not change the emission constant of gold substantially because platinum was evaporated last in contrast to Expt. I. The emission constant of platinum after sintering is even lower than before, again in contrast to Expt. I.

Expt. III. Simultaneously deposited metals. After our preliminary experiments in phototube (I), Expts. III were carried out in phototube (II). In this tube the alloy films were prepared by simultaneous deposition on a cathode cooled by liquid nitrogen. Immediately after deposition of the alloy film, the cathode was heated at room temperature and the spectral distribution curve was measured. The work functions calculated from them are given as ϕ_{fresh} in Table 3. Subsequently, the film was equilibrated by heating the cathode at 300°C. The method of simultaneous evaporation has the advantage that the gold and platinum atoms are brought into the vicinity of each other. This does not necessarily imply that a metastable solid solution with random distribution of the atoms is formed, as will be explained in part 4. But for those compositions outside the miscibility gap where a solid solution is stable, it may be expected that this solution is formed *in situ* by the present technique and that it will remain almost unaltered.

In Fig. 7 a rather pronounced minimum occurs at the gold-rich side at about 20 at. % Pt, whereas all other values lie on a gradually increasing line from gold to

TABLE 3
EXPT. III. SIMULTANEOUSLY EVAPORATED Pt–Au ALLOYS; THE WORK FUNCTION[a]

			After CO-admission					
Pt (at. %)	ϕ_{fresh} (eV)	$\phi_{sintered}$	A	B	C	D	E	F
0	5.41	5.38	5.39	5.40	5.41	5.42	5.43	5.37
15	5.42	5.34	5.35	—	—	5.41	5.43	5.35
20	5.35	5.34	5.35	5.37	5.37	5.41	5.43	5.35
25	5.36	5.34	5.34	—	—	5.40	5.44	5.35
31	5.37	5.34	5.35	5.37	5.38	5.42	5.45	5.34
40	5.38	5.34	5.35	—	5.39	5.42	5.45	5.35
51	5.41	5.34	5.35	5.38	5.39	5.43	5.45	5.35
59	5.44	5.34	5.36	5.38	—	5.45	5.48	5.34
66	5.48	5.35	5.37	5.39	5.42	5.47	5.49	5.34
73	5.52	5.35	5.38	—	—	5.49	5.50	5.34
79	5.56	5.36	5.39	5.42	5.45	5.50	5.51	5.35
84	5.59	5.37	5.41	—	5.46	5.52	5.52	5.36
88	5.58	5.38	5.43	5.45	5.48	5.51	5.53	5.34
100	5.64	5.72	5.75	5.75	5.75	5.75	5.75	5.73

[a] Legend: A = after 1 day under 10^{-5}–10^{-4} Torr CO at ambient temperature; B = after 2 days under 10^{-5}–10^{-4} Torr CO at ambient temperature; C = after 4 days under 10^{-5}–10^{-4} Torr CO at ambient temperature; D = after 16 hr under 10^{-5}–10^{-4} Torr CO at 100°C; E = after 80 hr under 10^{-5}–10^{-4} Torr CO at 100°C; and F = after pumping and heating at 300°C during 16 hr.

platinum. A small dip in the curve at 90 at. % Pt might indicate the *in situ* presence of an appreciable amount of the stable, platinum-rich composition in the surface area irradiated by the light beam. After sintering at 300°C during 2 hr the work functions of the alloys appear to be located on a plateau having a value of 5.34–5.37 eV for a bulk composition from 10 to 90 at. % Pt. It is noteworthy that the alloys now possess work functions lower than that of either pure metal and that the value of the plateau coincides with the value of the minimum at 20 at. % Pt of the fresh film.

Expt. IV. Chemisorption of carbon monoxide. After equilibration of the film of Expt. III carbon monoxide was admitted

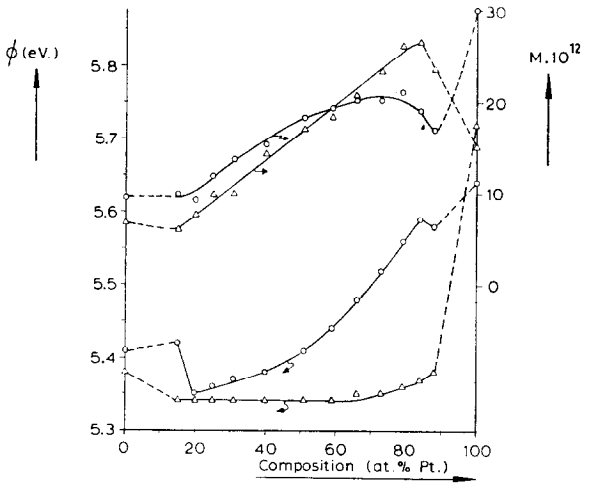

FIG. 7. The work functions (lower curves), and emission constants (upper curves) of a film prepared by simultaneous deposition of the metals (Expt. III): ○, fresh films; △, film after sintering at 300°C.

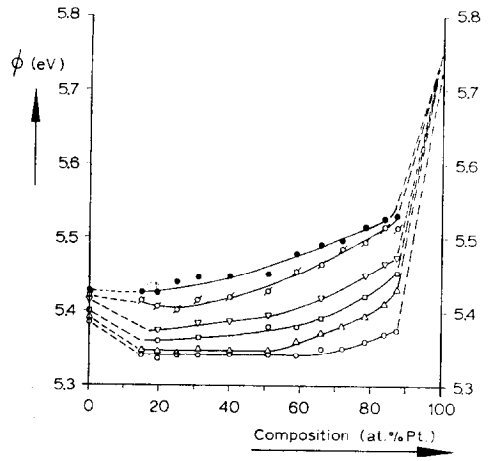

FIG. 8. The work functions of an equilibrated alloy film after treatments with CO (Expt. IV): ○, film sintered at 300°C; △, after 16-hr exposure to 10^{-4} Torr CO at 20°C; □, after 40-hr exposure to 10^{-4} Torr CO at 20°C; ▽, after 90-hr exposure to 10^{-4} Torr CO at 20°C; ◌, after 16-hr exposure to 10^{-4} Torr CO at 100°C; ●, after 80-hr exposure to 10^{-4} Torr CO at 100°C.

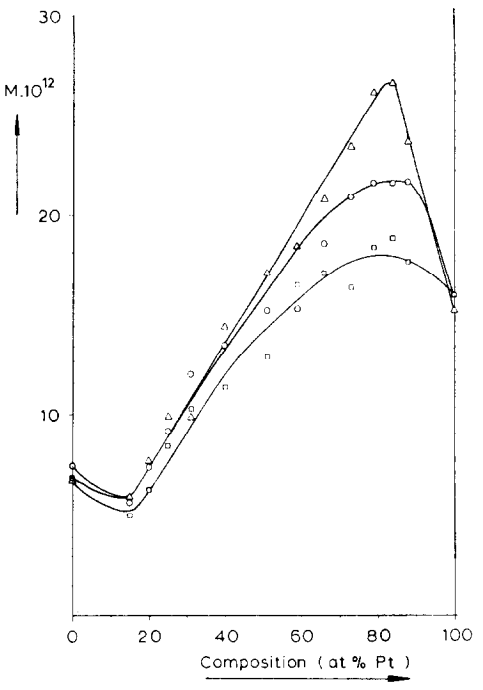

FIG. 9. The emission constants of an equilibrated alloy film after treatments with CO (expt. IV): △, film sintered at 300°C; ○, after 90-hr exposure to 10^{-4} Torr CO at 20°C; □, after 80-hr exposure to 10^{-4} Torr CO at 100°C.

for reasons given in the Introduction. The results shown in Table 3 and Fig. 8 were as follows: Immediately after admission of CO, no appreciable change of the work function of gold and the alloys was observed, while ϕ_{Pt} was raised by about 0.03 eV. Upon maintaining the film under a pressure of about 10^{-5}–10^{-4} Torr CO during 1, 2, and 4 days, respectively, the work function of all alloys slowly increased. After 1 day this increase was observed in the platinum-rich region only. During subsequent days, the work function increase also penetrated to the more gold-rich part of the film.

Obviously, a slow diffusion process is responsible for this phenomenon. This conclusion was confirmed by increasing the temperature to a value which favors the rate of diffusion in the solid state substantially, without breaking the Pt–CO bonds (*18*, *19*). Figure 8 shows that a considerable increase of the work functions was caused by a treatment at 100°C during comparatively short periods of time. The change of the emission constants differs markedly from former experiments (Fig. 9). As the major proportion of carbon monoxide is desorbed from platinum at 300°C (*18*, *19*), one may expect that upon heating at 300°C and pumping, the original plateau would be regained. This expectation was indeed confirmed by the results shown in Table 2 and Fig. 10.

4. Discussion

From Expts. I and II it became clear that the interdiffusion of gold and platinum is much slower than that of copper and nickel. This is in agreement with diffusion data from Jost (*20*). From the well-known relation for the diffusion coefficient D:

$$D = D_0 \cdot e^{-Q/RT}$$

wherein $D_0 = 1.24 \times 10^{-3}$ cm²/sec and the activation energy of diffusion $Q = 39.0$ kcal/g-atom, as reported for the diffusion of platinum in gold between 740 and 986°C, it was calculated by using Fick's law that the average displacement of platinum atoms per hour will be of the order of 1 Å

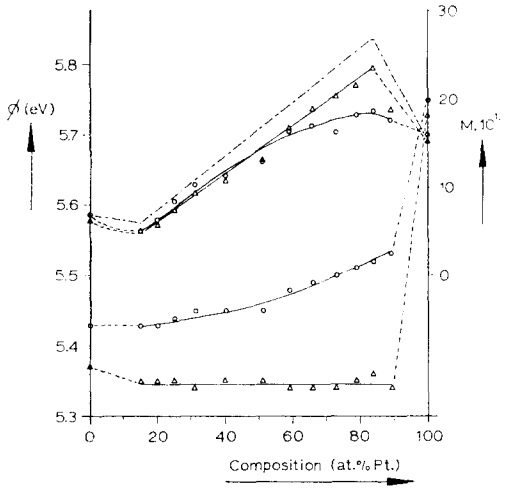

FIG. 10. Re-equilibration of the CO-treated alloy film (Expt. IV): ○, final stage of CO-treatment; △, after pumping at 300°C.

at 200°C and of the order of 10 Å at 300°C. The changes in the work functions of Expt. II are more pronounced than in Expt. I. This is in agreement with the fact that the diffusion of gold into platinum is a faster process than in the reverse direction. The findings with respect to lateral diffusion of gold over platinum support this conclusion. The partial minima occurring at the gold-rich side for Expts. I and II are ascribed to the fast formation of a gold-rich alloy while the neighboring segments are still far from equilibrium. A further argument for this explanation is provided by results of Expt. III: in Fig. 7, the partial minimum for the film deposited simultaneously at liquid nitrogen, and subsequently sintered at room temperature, lies at about the same level as the plateau of the alloys equilibrated after sintering at 300°C. It seems, therefore, that the sintered films of Expts. I and II were far from equilibrium, while the sintered film of Expt. III was equilibrated.

The maximum shown in Figs. 6 and 7 is not representative for all measurements. The peculiar values found near the edges of the photocathode, especially at the platinum-rich side, however, always disappeared after sintering. It seems plausible to assume that premature sintering of segments near the platinum source might cause a local maximum of the work function.

The results from Expt. III are in agreement with our stated expectation: The Pt–Au system behaves in a manner analogous to the Ni–Cu system. The kinetic energy of the impinging metal atoms in combination with the lattice energy liberated by each condensing atom and the heat of radiation emitted from the evaporation sources will enable the growing film to acquire an atomic arrangement which is somewhere in between the metastable state of a random distribution and the thermodynamically stable state of two coexisting alloys of different composition. We visualize that separate clusters of gold-rich and platinum-rich nuclei are formed. The gradually increasing work function from gold-rich alloys up to Pt-rich alloys may be explained by representing a surface containing both platinum and gold in about the same proportions as represented on the abscissa. During sintering an accelerated interdiffusion of the clusters takes place by relatively rapid surface diffusion, migration along the boundaries of neighboring crystallites and by the relatively slow volume diffusion. Gold having the highest mobility, the lowest surface tension and in relation to platinum, a pronounced Kirkendall effect will diffuse rapidly over the platinum clusters by surface diffusion and grain boundary diffusion.

Our lateral diffusion data are in agreement with this assumption. After and to some extent during the surface migration of gold, the composite clusters consisting a platinum kernel and a gold skin, will equilibrate by volume diffusion. This process comes to an end after formation of the stable gold-rich or platinum-rich alloys. For those compositions where the phase diagram predicts only one single phase rich in platinum, an enrichment of the surface with gold is still possible because in this way the surface energy may be lowered. This follows from the values of the surface tensions which are for gold and platinum 754 (*21*) and 1885 (*22*) dynes/cm respectively (measured at their respective melting points).

Adsorbed carbon monoxide raises the work function of platinum by 0.03 eV. This result is at variance with the contact potential values of Dorgelo and Sachtler (*23*) (+0.23 eV), the field emission data of Rootsaert *et al.* (*15*) (+0.68 eV) and the field emission data of Lewis and Gomer (*18*) (+0.4 eV). However, our photoelectric results on pure platinum, which will be described more extensively (*24*), are in reasonable agreement with the static capacitor data of Heyne and Tompkins (*25*) who reported a change of the surface potential of 0 ± 0.01 eV on polycrystalline platinum films.

This small effect of CO on the work function of platinum severely limits the usefulness of CO for chemisorptive titration of platinum-containing gold surfaces. The result that the work function of our alloys was found unchanged within the experimental error (± 0.005 eV for a single Fowler plot) after short exposure to carbon monoxide gas therefore permits only the semiquantitative expectation that the platinum content of these surfaces must have been less than about 17 at. %.

The slow phenomena observed after exposure to CO for extended periods of time are, however, remarkable; these may be summarized as follows:

1. The work function slowly increases over a period of days. The highest rate of increase is observed at the most platinum-rich side of the plateau.

2. The emission constants of the alloy change gradually with time (for the sake of clarity, only three curves are shown in Fig. 9).

3. Upon heating at a moderately high temperature (100°C) the effects described in (1) and (2) are accelerated and completed.

4. After heating at 300°C while pumping off the carbon monoxide, the work function of the alloys return almost exactly to their original values and the shape of the emission constant curve changes to its original shape and almost to its original position (Fig. 10). We interpret these phenomena by assuming that in the presence of CO gas, the alloy surfaces become slowly enriched with platinum, as predicted in the Introduction. Even the shape of the curves in Fig. 8 can be explained in this way. In the platinum-rich region on the photocathode, the crystallites consist of a rather thick platinum-rich kernel surrounded by a thin gold-rich skin, whereas the crystallites in the gold-rich region comprise relatively thick gold-rich jackets around a minor platinum-rich kernel. The path of diffusion, therefore, for Pt-atoms from the kernel to the surface is shorter for the platinum-rich film segments than for the gold-rich side. As soon as a Pt-atom has arrived at the surface a new bond is formed with an impinging CO-molecule preventing diffusion of this Pt-atom back into the interior. It is obvious that the diffusion process will be faster at higher temperature as was found experimentally.

It may be that the process of thermal diffusion of a Pt-atom from the interior to the surface is accelerated by lattice defects injected into the subsurface zone by the phenomenon of corrosive chemisorption (*26*). As the heat of adsorption of CO on platinum (*15*, *16*) is at least 30 kcal $mole^{-1}$, the existence of corrosive chemisorption in this case (*24*) is possible. The behavior of the emission constant (Fig. 9) indicates that bulk-effects become more involved during the course of the treatment of CO. According to the bulk diffusion data of Jost (*20*), Pt-atoms can diffuse through gold only over distances of less than 10^{-3} Å/hr at 20°C. As the changes found by us are much faster it is not unlikely that corrosive chemisorption of CO is involved in this process of migration of Pt-atoms from the bulk to the surface.

5. Conclusions

The equilibration model developed on the basis of the copper–nickel alloy system, showing a miscibility gap in the solid state, is valid also for the platinum–gold system. The model, therefore, appears to be representative for the equilibration of alloys possessing a miscibility gap and being composed of metals having considerably different diffusion rates. The rate of equilibration depends on the temperature and the

length of the diffusion path. For the Au–Pt system only simultaneously evaporated alloys were able to reach equilibrium at 300°C within a reasonable period of time. The work function of equilibrated Au–Pt alloys all lie below that of each of the pure metals. This, again, is analogous to the copper–nickel system. Although minima in the work function were reported also for other alloys (*27–32*), we are unable to say to what extent this phenomenon may be generalized. In the case of K–Na alloys, Van Oirschot (*33*) did not observe a minimum in the work function.

The results further show that the surface composition of an alloy strongly depends on the contacting gas. Chemisorption of carbon monoxide induces a rearrangement of the metal atoms in the equilibrated alloy films, resulting in an increased Pt/Au ratio at the surface. The major proportion of the CO–Pt bonds are broken at 300°C; by pumping CO at that temperature the Pt/Au ratio of the surface returns to the value prior to admission of CO.

Acknowledgments

The investigations were supported by the Netherlands Foundation for Chemical Research (SON) with financial aid from the Netherlands Organization for the Advancement of Pure Research (ZWO). The authors are indebted to Mr. F. C. Kauffeld for skillfully developing and constructing the phototubes.

References

1. Sachtler, W. M. H., and Dorgelo, G. J. H., *J. Catal.* **4**, 654 (1965).
2. Sachtler, W. M. H., and Jongepier, R., *J. Catal.* **4**, 665 (1965).
3. Sachtler, W. M. H., Dorgelo, G. J. H., and Jongepier, R., *Proc. Int. Symp. Basic Problems Thin Film Phys., Clausthal, 1965.*
4. Van der Plank, P., thesis, Leyden University, the Netherlands, 1968.
5. Van der Plank, P., and Sachtler, W. M. H., *J. Catal.* **12**, 35 (1968).
6. Vecher, A. A., and Gerasimov, Y. I., *Russ. J. Phys. Chem.* **37**, 254 (1963).
7. Rapp, R. A., and Maak, F., *Acta Met.* **10**, 62 (1962).
8. Seith, W., and Kottmann, A., *Angew. Chem.* **64**, 379 (1952).
9. Trønsdal, G. O., and Sørum, H., *Phys. Status Solidi* **4**, 493 (1964).
10. Cadenhead, D. A., and Wagner, N. J., *J. Phys. Chem.* **72**, 2775 (1968).
11. Darling, A. S., Mintern, R. A., and Chaston, J. C., *J. Inst. Met.* **81**, 125 (1952).
12. Van den Toorn, L. J., thesis, Technical University, Delft, the Netherlands, 1960.
13. Bolk, A., *Acta Met.* **9**, 632 (1961).
14. Bolk, A., *Acta Met.* **9**, 643 (1961).
15. Rootsaert, W. J. M., Van Reyen, L. L., and Sachtler, W. M. H., *J. Catal.* **1**, 416 (1962).
16. Brennan, D., and Hayes, F. H., *Phil. Trans. Roy. Soc. London, Ser. A* **258**, 347 (1965).
17. Hall, W. K., *J. Catal.* **6**, 314 (1966).
18. Lewis, R., and Gomer, R., *Nuovo Cimento, Suppl.* **V, 2**, 506 (1967).
19. Morgan, A. E., and Somorjai, G. A., *Surface Sci.* **12**, 405 (1968).
20. Jost, W., *Z. Phys. Chem. Abt. B* **21**, 158 (1933).
21. Smirnova, V. I., Ormont, B. F., *Zh. Fiz. Khim.* **33**, 771 (1959).
22. Allen, R., *Trans. AIME* **227**, 1175 (1963).
23. Dorgelo, G. J. H., and Sachtler, W. M. H., *Naturwissenschaften* **46**, 576 (1959).
24. Bouwman, R., Van Keulen, H. P., and Sachtler, W. M. H., *Ber. Bunsenges. Phys. Chem.* **74**, 198 (1970).
25. Heyne, H., and Tompkins, F. C., *Proc. Roy. Soc., Ser. A* **292**, 460 (1966).
26. Sachtler, W. M. H., *Angew. Chem. int. Ed. Engl.* **7**, 9 (1968).
27. Dyubua, M. L., Kultashev, O. K., and Gorshkova, L. V., *Sov. Phys. Solid State* **8**, 882 (1966).
28. Gurov, K. P., and Pekarev, A. I., *Fiz. Metal. Metalloved.* **17**, 500 (1964).
29. Dyubua, B. C., Kultashev, O. K., and Tsyganova, I. A., *Radiotekh. Elektron.* **9**, 2061 (1964).
30. Pines, B. Y., *Zh. Tekh. Fiz.* **22**, 1908 (1952).
31. Dyubua, B. C., and Kultashev, O. K., *Fiz. Metal. Metalloved.* **21**, 396 (1966).
32. Dyubua, B. C., Pekarev, A. I., Popov, B. N., and Tylkina, M. A., *Radiotekh. Elektron.* **7**, 1566 (1962).
33. Van Oirschot, T. G. J., *Thesis*, Leyden University, the Netherlands, (1970).